# Laboratory Design of Representative Real Shallow Basins for Validation of Numerical Models

EL Mehdi CHAGDALI[1], Cédric GOEURY[1], Benjamin DEWALS[2], Sébastien ERPICUM[2], Matthieu SECHER[3], Kamal EL KADI ABDEREZZAK[1]

[1] National Laboratory for Hydraulics and Environment (LNHE), EDF R&D, France
el-mehdi.chagdali@edf.fr
cedric.goeury@edf.fr
kamal.el-kadi-abderrezzak@edf.fr

[2] Research Group of Hydraulics in Environmental and Civil Engineering (HECE), University of Liège, Belgium
b.dewals@uliege.be
s.erpicum@uliege.be

[3] EDF Hydro-CIH, France
Matthieu.secher@edf.fr

ABSTRACT

Shallow reservoirs are hydraulic engineering structures widely used for trapping sediments or storing water. Several research works focused on the links between reservoir geometry, boundary conditions and flow patterns but considered simplified configurations. The objective of this study is to complete the existing data by designing a set of new laboratory configurations representative of a range of real cases to get new data for the validation of numerical models and to allow a better understanding of the physics. Two inlet flow configurations are considered with rectangular reservoirs: an open channel (reference case), and a pressurized flow jet; the outlet is a free surface channel for both configurations. A wide range of parameters extracted from real reservoirs are investigated. Parameters with significant impact on the flow pattern are analyzed and retained for the design of laboratory experiences (Reynolds number, Froude number, Friction number…). A numerical pre-simulation is performed with the TELEMAC-3D code to test the hydraulic parameters and establish a preliminary numerical comparison between the reference and jet cases. The 3D results and 2D average results of velocity magnitude extracted from TELAMAC-3D simulations are presented and compared. For the same hydraulic conditions, comparisons between the reference and jet cases show a different flow pattern and distribution.

## 1. Introduction

Shallow reservoirs are hydraulic structures widely used for trapping sediments or storing water. The loss of the effective storage volume due to sedimentation decreases the reservoir functionality for flood control, hydropower generation, irrigation, water supply and reactional activities (Schleiss et al., 2016). The flow pattern and trap efficiency of a shallow reservoir depend on its geometrical shape, hydraulic conditions, boundary conditions (i.e. inlet and outlet), and sediment characteristics (Kantoush, 2008; Camnasio et al., 2013). hydro-morphodynamic numerical models are useful tools for optimizing the design of shallow reservoirs and predicting their performance.

The first experimental studies on shallow reservoirs concerned the effect of a sudden expansion through an inlet free surface channel for a rectangular reservoir. Abbott and Kline (1962) were amongst the firsts to study this subject. The rectangular reservoir was considered with infinite length and results showed the presence of three regions: a first region at the immediate inlet of the reservoir with a three-dimensional stationary recirculation, a two-dimensional stationary region with a point of attachment downstream from the first region, and an unsteady tail region downstream from the second region. For turbulent flow, there was no effect of tested Reynolds number on the length of the three zones. Durst et al. (1974) showed that the flow after a sudden expansion was three-dimensional, while Cherdron et al. (1978) showed that the flow at low Reynolds number was nominally two-dimensional. Durst et al. (1974) and Cherdron et al. (1978) also explained the effect of the Reynolds number on the flow typology. For low Reynolds number, a symmetrical flow was found. For higher Reynolds number, an asymmetry was found that was explained by the small perturbations created at the expansion level. These perturbations are involved in the shear layer created between the main flow and the

recirculation in the reservoir corner. As a continuation on the work on sudden expansion through an inlet free surface channel, Mizushima and Shiotani (2001) evaluated the effect of a downstream contraction combined with an upstream expansion at the basin entrance. The inlet and outlet channels were of the same width. Authors found that the addition of the downstream contraction restabilized the symmetric state of the flow.

Kantoush (2008) studied the flow pattern in different shallow rectangular reservoirs with free surface channels at the inlet and outlet. Starting with a reference reservoir, the length was gradually reduced while keeping a fixed width. Conversely, while keeping a fixed length, the width was modified. Different ranges of Reynolds number and Froude number were studied. Dissymmetric flows were observed for some configurations despite of the symmetry of the reservoir. Kantoush (2008) identified four types of flows: symmetrical with two attachment points, asymmetrical with two attachment points, symmetrical with one attachment point, and symmetrical with no reattachment point. Kantoush (2008) also studied gradually expanding reservoirs with one lozenge, one hexagon and one rectangular shape with reduced inlet angles. Dufresne et al. (2010) clarified the transition between symmetric and asymmetric flows in rectangular reservoirs using the shape factor defined as $SF = L_1/(\Delta B^{0.6} b^{0.4})$, with $L_1$ the reservoir length, $b$ the inlet channel width, and $\Delta B = (B - b)/2$ the width of the sudden expansion with $B$ as the reservoir width. It appears that symmetric flows occur for $SF < 6.2$ and asymmetric flows take place for $SF > 6.8$. Camnasio et al. (2013) confirmed experimentally the impact of varying the position of the channel inlet and outlet on the velocity field and sedimentation. Choufi et al. (2014) examined the effect of bottom roughness of a shallow rectangular reservoir with variable geometry and symmetrical inlet and outlet on the flow field. Asymmetric flows could be developed depending on certain edge conditions, resulting from the growth of small perturbations in initial and boundary conditions. Peltier et al. (2014) investigated oscillatory flows of "meandering jet" type in about 50 experiments performed in rectangular reservoirs. The frequency, wavelength and lateral extension of the flow were extracted from Large Scale Particle Image Velocimetry (LSPIV) measurements using a Proper Orthogonal Decomposition (POD). Threshold values on the shape factor and on the Froude number were identified to predict the occurrence of a meandering jet type flow. Relationships were obtained between the characteristics of the meandering jet and friction number S, which was defined by Peltier et al. (2014) as $S = \lambda \Delta B/(8H)$ with H the water depth and $\lambda$ the friction coefficient.

Some authors were interested on inlet boundary conditions with turbulent circular jet. Stovin and Saul (1994) performed a series of experiments on a rectangular reservoir whose inlet and outlet were circular pipes. Adamsson et al. (2005) performed an experimental study on a large basin (i.e. 13 m long and 9 m wide and 0.8 m high); the inlet was a circular jet with a diameter of 0.23 m and the outlet was a weir. Two large symmetrical recirculations were observed. Dufresne (2008) conducted 55 experiments in a rectangular reservoir with a circular pipe at the inlet and a frontal weir at the outlet. He observed an asymmetrical and stationary flow for low water heights and a symmetrical and stationary flow for higher water heights. A pseudo periodic regime appeared between these two cases. In a broader context than shallow reservoirs, Jirka (2004) showed that jet behavior in ambient water bodies is highly dependent on the initial flow conditions, such as initial volume, momentum and buoyancy fluxes, and discharge angle. Concerning real cases, the analysis of shallow reservoirs managed by EDF Hydro-CIH showed an important difference within their geometries, boundary conditions (e.g. free surface channel, jet, gate, weir) and hydro-morphodynamic conditions (Claude et al., 2019). Table 1 summarizes the characteristics of boundary conditions in reservoirs of interest.

**Table 1.** Boundary conditions characteristics of real cases

| Reservoirs | Inlet boundary | | | Outlet boundary | | |
|---|---|---|---|---|---|---|
| | Type | Number | Position | Type | Number | Position |
| Cheylas | Pressurized jet (plant outtake gallery) | 1 | Inside | Flap gate<br>Pressurized water intake (plant intake gallery) | 3<br>1 | Lateral wall<br>Inside |
| Longefan | Free surface channel | 1 | Corner | Weir | 1 | Corner |
| Cadarache | Radial gates | 2 | Lateral wall | Weir | 1 | Lateral wall |
| La Coche | Pressurized jet (plant outtake gallery + water supply gallery) | 2 | Lateral wall | Pressurized water intake (plant intake gallery) | 1 | Inside |

Existing experimental works depicted above show certain limitations in terms of engineering needs, as they mainly focused on simple rectangular reservoirs with inlet and outlet rectangular free surface boundary channels, generally situated on opposite sides, and in a lesser degree, some experiences with inlet turbulent jet. On the other hand, real reservoirs feature different characteristics of boundary conditions (Table 1). The objective of this study is to design a set of new laboratory configurations representative of a wide range of real cases, complementary to existing studies, which will allow the validation of numerical models, such as the widely used suite of TELEMAC-MASCARET codes (www.opentelemac.org). We are firstly interested in a comparison between two configurations: a "Reference case" with rectangular free surface channels at the inlet and outlet, and a "Jet case" with a free turbulent circular jet at the inlet boundary and free surface rectangular channel at the outlet. Then, an experimental design is set to study, from different geometrical perspectives, the turbulent jet as inlet boundary condition. A wide range of parameters extracted from real reservoirs are investigated (Reynolds number, Froude number, Friction number.). A numerical pre-simulation is performed using the TELEMAC-3D code for the reference and jet cases.

## 2. Choice of parameters and experimental design

The physical model was constructed in the laboratory of Hydraulics in Environmental and Civil Engineering (HECE) group at Liege University (Belgium), based on the facility widely used by Dufresne et al. (2010) and Peltier et al. (2014). The reservoir geometries that will be investigated have to fit in an existing horizontal flume (Fig. 1), $L$ = 10.4 m long, $B$ = 0.985 m wide and $h$ = 0.5 m deep. Considering a safety margin of 5 cm, the maximum water depth is about 0.45 m. The flume bottom and walls are fixed and made of glass. The reservoir width is equal to the flume width and the downstream and upstream extremities are created by solid blocks placed in the flume. The position of these blocks can be modified to change the reservoir length $L_1$. The inlet and outlet are located on opposite sides of the reservoir. The width of outlet boundary is fixed at $b_o$ = 0.08 m for all configurations. Regarding the pump characteristics, the flow rate that can be used is in the range 0.0002 to 0.006 $m^3/s$.

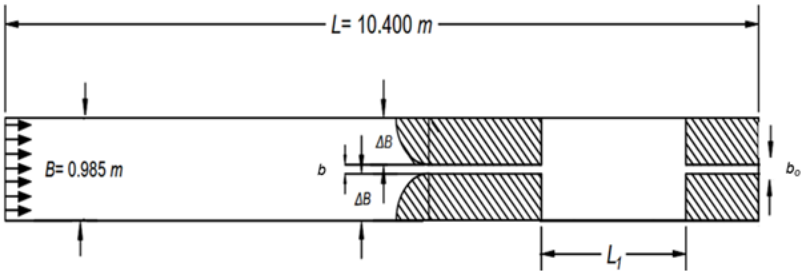


**Fig. 1.** Sketch illustrating the existing experimental flume at HECE laboratory, University of Liège (not to scale).

Following Peltier et al. (2014) the flow is be governed by eight parameters, namely reservoir length $L_1$, reservoir width $B$, inlet channel width or jet diameter $b$, flow depth $H$, mean depth-averaged velocity in the inlet channel $U$, roughness height $k_s$, kinematic viscosity $\nu$, and gravitational acceleration $g$. The velocity is calculated as $U = Q/(bH)$, with $Q$ the inlet flow rate. According to Vaschy Buckingham theorem, six dimensionless parameters can be defined: lateral expansion ratio $B/b$, length-to-width ratio $L/B$, flow depth-to-width ratio (i.e. shallowness parameter) $H/B$, Froude number $\mathsf{F} = U/(gH)^{1/2}$, Reynolds number $\mathsf{R} = 4UH/\nu$, and Friction number $\mathsf{S} = \lambda B/H$. In this later number, the friction coefficient $\lambda$ is a function of the relative roughness $k_s/H$ and Reynolds number R. The friction number is defined differently from Peltier et al. (2014). The width of the sudden expansion $\Delta B$ would not be available for real cases due to asymmetry of their boundary condition positions, the friction number S is therefore defined in terms of the reservoir width $B$.

Couples of points (S, F) are presented in Fig. 2 for real reservoirs with free surface inlet (Longefan and Cadarache), real reservoirs with inlet pressurized jet (Cheylas and La Coche), laboratory experiments with free surface inlet channel, and laboratory experiments with inlet jet. The Min and Max values correspond to minimum and maximum hydraulic operating values, respectively. For each reservoir S and F are calculated using the formulas detailed upper. For real reservoirs, the roughness height $k_s$ is calculated from the median sediment grain size $D_{50}$ and sensitivity analysis is done while taking a minimum value of $k_s = D_{50}$ and maximum value of $k_s = 100D_{50}$; the error bar in the scatter plot displays the confidence interval for the Friction number. The objective is to determine experimental values of $Q$, $b$ and $H$ that will allow reaching minimal and maximal values of Friction and Froude numbers to encompass the couple of points (S, F) in the scatter plot while considering experimental constraints.

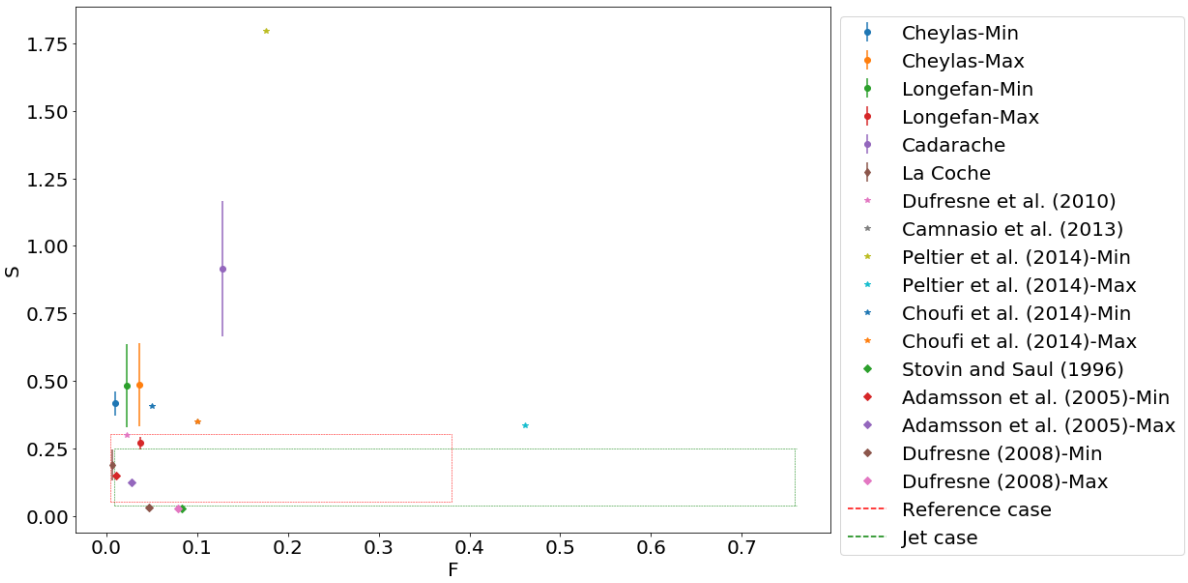


**Fig. 2.** Friction factor S in terms of Froude number F for real reservoirs, laboratory experiments, limits for reference and jet cases.

To allow future comparisons, the same values of $H$ and $Q$ are set for both reference and jet cases, recalling that the flow rate $Q$ is between 0.0002 and 0.006 $m^3/s$ and the Froude number F should be set lower than 1 to remain in subcritical flow regime. The tested values for $Q$, $b$ and $H$ for the jet case showed that the constraining limits to encompass a higher number of points is the upper limit of S; the lower limit of S can be obtained for $H$ = 0.30 m. Highest values of S could be reached for lowest values of $H$, because of the increase in shallowness parameter and friction coefficient. The lowest value of $H$ is in turn limited by the jet diameter, in order to ensure a desired condition of $H = 2.5b$. Considering the experimental constraints, $b$ = 0.04 m is set for jet case, which implies the following lowest flow depth $H$ = 0.1 m. Concerning the reference case, the blocks used in Peltier et al.'s (2014) experiments will be reused for operational convenience, which yields inlet channel width of $b$ = 0.08 m. Table 2 summarizes the selected parameters retained for the reference and jet cases. Figure 2 shows that experimental jet limits encompass the existing experiences in the literature using jet as inlet boundary condition and La Coche real reservoir. Table 3 summarizes the geometrical parameters retained for this study. For each case, a short reservoir and long reservoir will be studied.

**Table 2.** Selected parameters for reference and jet cases

| | Configuration Number | $b$ (m) | $b_o$ (m) | $H$ (m) | $Q$ ($m^3/s$) | $U$ (m/s) | R | F |
|---|---|---|---|---|---|---|---|---|
| Reference case | 1 | 0.08 | 0.08 | 0.10 | 0.0002 | 0.025 | $1.00 \times 10^4$ | 0.025 |
| | 2 | 0.08 | 0.08 | 0.10 | 0.0030 | 0.375 | $1.50 \times 10^5$ | 0.378 |
| | 3 | 0.08 | 0.08 | 0.30 | 0.0060 | 0.250 | $3.00 \times 10^5$ | 0.146 |
| | 4 | 0.08 | 0.08 | 0.30 | 0.0002 | 0.008 | $1.00 \times 10^4$ | 0.005 |
| Jet case | 5 | 0.04 | 0.08 | 0.10 | 0.0002 | 0.050 | $2.00 \times 10^4$ | 0.050 |
| | 6 | 0.04 | 0.08 | 0.10 | 0.0030 | 0.750 | $3.00 \times 10^5$ | 0.757 |
| | 7 | 0.04 | 0.08 | 0.30 | 0.0060 | 0.500 | $6.00 \times 10^5$ | 0.300 |
| | 8 | 0.04 | 0.08 | 0.30 | 0.0002 | 0.017 | $2.00 \times 10^4$ | 0.010 |

**Table 3.** Geometrical parameters for reference and jet cases

| Case | $L_1$ (m) | $\Delta B$ (m) | $b$ (m) | Shape factor (SF) |
|---|---|---|---|---|
| Reference case | 2.00 | 0.45 | 0.08 | 8.87 (Long reservoir) |
| | 1.05 | 0.45 | 0.08 | 4.65 (Short reservoir) |
| Jet case | 2.00 | 0.47 | 0.04 | 11.4 (Long reservoir) |
| | 1.05 | 0.47 | 0.04 | 5.98 (Short reservoir) |

The purpose of this experimental design is firstly to compare the jet and rectangular cases and then to have a clear description on different configurations of jet behavior that will allow a proper validation of numerical model. The geometrical configurations are detailed in Table 4. For each configuration, four hydraulic conditions will be studied (Table 2). For each case, a short and a long reservoir will be designed (Table 3). The effect of the inlet jet will be compared to the reference case for the four hydraulic conditions set previously. Thereafter, and because of asymmetry of boundary conditions in real cases, different positions of the jet will be tested. For the case of jet at the center position, different exit angles will be studied.

**Table 4.** Geometrical parameters for experimental set-up

| $L_1$ (m) | $\Delta b$ (m) | $b$ (m) | Inlet boundary conditions | Reservoir type | Jet position | Jet angle (°) with respect to $X$ axis at horizontal plan |
|---|---|---|---|---|---|---|
| 2.00 | 0.45 | 0.08 | Rectangular channel | Long reservoir | - | - |
| 1.05 | 0.45 | 0.08 | Rectangular channel | Short reservoir | - | - |
| 2.00 | 0.47 | 0.04 | Jet | Long reservoir | Center | 0 |
| 1.05 | 0.47 | 0.04 | Jet | Short reservoir | Center | 0 |
| 2.00 | - | 0.04 | Jet | Long reservoir | Right side | 0 |
| 1.05 | - | 0.04 | Jet | Short reservoir | Right side | 0 |
| 2.00 | - | 0.04 | Jet | Long reservoir | Left side | 0 |
| 1.05 | - | 0.04 | Jet | Short reservoir | Left side | 0 |
| 2.00 | - | 0.04 | Jet | Long reservoir | Downstream from center | 0 |
| 1.05 | - | 0.04 | Jet | Short reservoir | Downstream from center | 0 |
| 2.00 | - | 0.04 | Jet | Long reservoir | Upstream from center | 0 |
| 1.05 | - | 0.04 | Jet | Short reservoir | Upstream from center | 0 |
| 2.00 | 0.47 | 0.04 | Jet | Long reservoir | Center | 30 |
| 1.05 | 0.47 | 0.04 | Jet | Short reservoir | Center | 30 |
| 2.00 | 0.47 | 0.04 | Jet | Long reservoir | Center | 45 |
| 1.05 | 0.47 | 0.04 | Jet | Short reservoir | Center | 45 |
| 2.00 | 0.47 | 0.04 | Jet | Long reservoir | Center | 60 |
| 1.05 | 0.47 | 0.04 | Jet | Short reservoir | Center | 60 |

## 3. Numerical pre-simulations

The turbulent jet could be divided into three regions: near field, intermediate field, and far field (Fischer et al., 1979). A model with small spatial and short time scales is necessary to accurately describe near-field mixing in the vicinity of the release point (Jirka, 2004). However, in the far field the behavior is dominated by ambient flow conditions that operate on much larger time and space scales. Numerical pre-simulations are performed with TELEMAC-3D numerical code to test hydraulic parameters chosen previously, and to establish a preliminary numerical comparison between reference and jet cases. TELEMAC-3D uses a sigma transformation on the vertical (non-conforming transformation) which facilitates the construction of a 3D mesh. This transformation allows having a structured mesh on the vertical, built as an extrusion of a 2D mesh along the vertical, then divided into layers. Unliked some CFD codes where it is possible to define CAD objects that allow representing the boundary conditions in a faithful way, it is not possible in TELEMAC-3D to represent these boundary conditions accurately. The method used here is the prescription of these conditions on several defined planes. Thus the prescribed flow is transformed into velocity condition on liquid boundary only on the specified planes, while velocities are set to zero otherwise. TELEMAC-3D is applied with non-hydrostatic pressure distribution, k–ε turbulence model in both horizontal and vertical directions, and LIPS (Locally semi-Implicit Predictor-corrector Scheme) for advection of velocity and turbulence. The Strickler formula is used for the friction term; a value of 80 $m^{1/3}$ $s^{-1}$ (corresponding to PVC) is retained for the bed and walls, which is equivalent to a roughness height $k_s$ = $10^{-3}$ mm. The 3D model is composed of seven layers uniformly distributed along the vertical, based on 2D unstructured mesh (0.004 m space step) with a total of 930 000 nodes. Figure 3 shows the 2D unstructured mesh and boundary condition positions for reference and jet cases. For the jet case, the inlet pipe is located horizontally at $x$ = 0 and - 0.02 m < $y$ < 0.02 m and, and vertically between plan 3 located at $z$ = 0.126 m and plan 4 located at $z$ = 0.168 m ($z$ = 0 is set at the reservoir bottom). Configurations 3 and 7 presented in Table 2 are simulated.

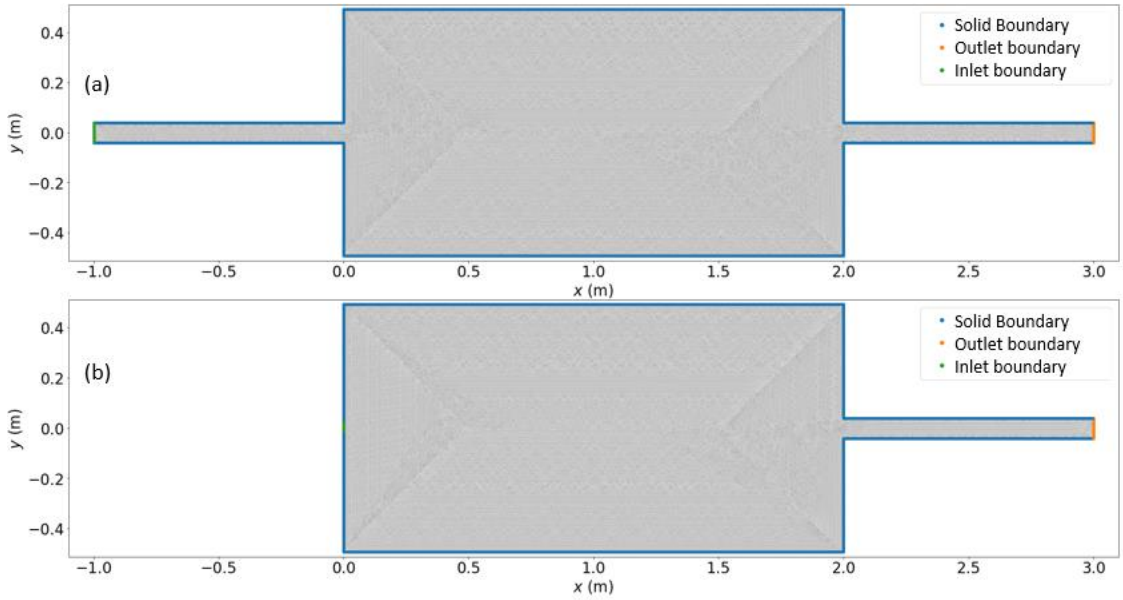


**Fig. 3.** Unstructured 2D mesh and boundary condition positions for (a) reference case, and (b) jet case (2D).

Figure 4 describes the 2D average velocity magnitude and streamlines at different time steps. The 2D average velocity magnitude of TELEMAC-3D simulations is compared for reference and jet cases. A steady state is found for the reference case with symmetrical pattern. The jet case yields an oscillatory flow pattern.

The 3D numerical results are analyzed while comparing velocity magnitude for reference and jet cases at $y$ = 0.0 m. The results show that velocity decreases along the reservoir for both cases (Fig. 5). The jet configuration does not spread along the water depth of the reservoir. The velocity magnitude is higher for jet case compared to reference case and is mainly localized in the jet direction.

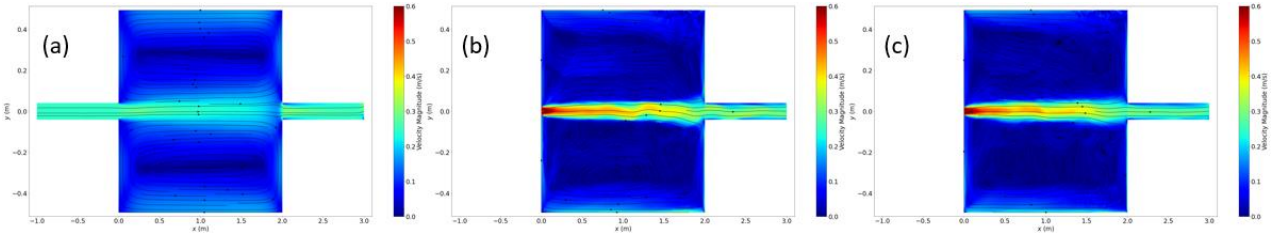


**Fig. 4.** Two-dimensional (2D) average velocity magnitude and streamlines for - (a) Steady state of reference case at t = 800 s, (b) Oscillatory state for jet case at t = 400 s, (c) Oscillatory state for jet case at t = 800 s.

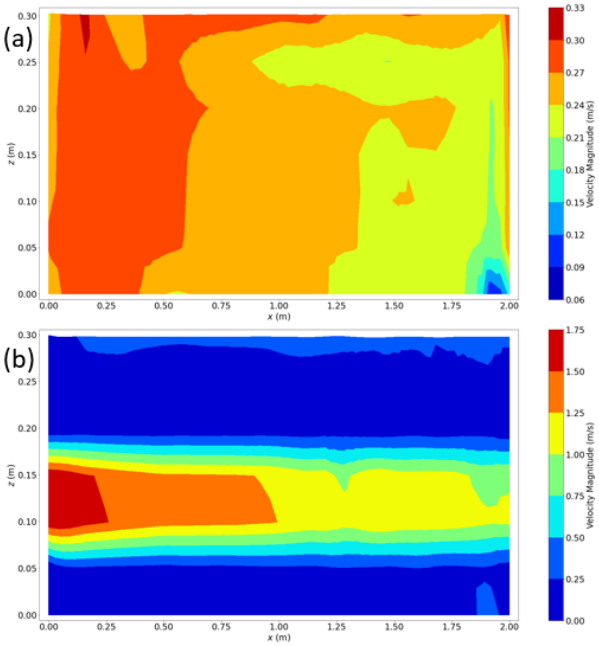


**Fig. 5.** Two-dimensional (2D) velocity magnitude withTELEMAC-3D numerical simulations for – (a) reference case and (b) jet case, at $y$ = 0.0 m. Note that the legend is not uniformized for reference and jet cases because of their different velocity magnitude values.

Figure 6 shows 2D velocity magnitude for reference and jet cases at $x$ = 0.1 m (just upstream of the inlet), $x$ = 1.0 m (middle) and $x$ = 2.0 m (reservoir outlet). The results confirm that the jet does not spread along the flow depth. For the same hydraulic conditions, a different flow pattern and distribution are found depending on the inlet flow configuration.

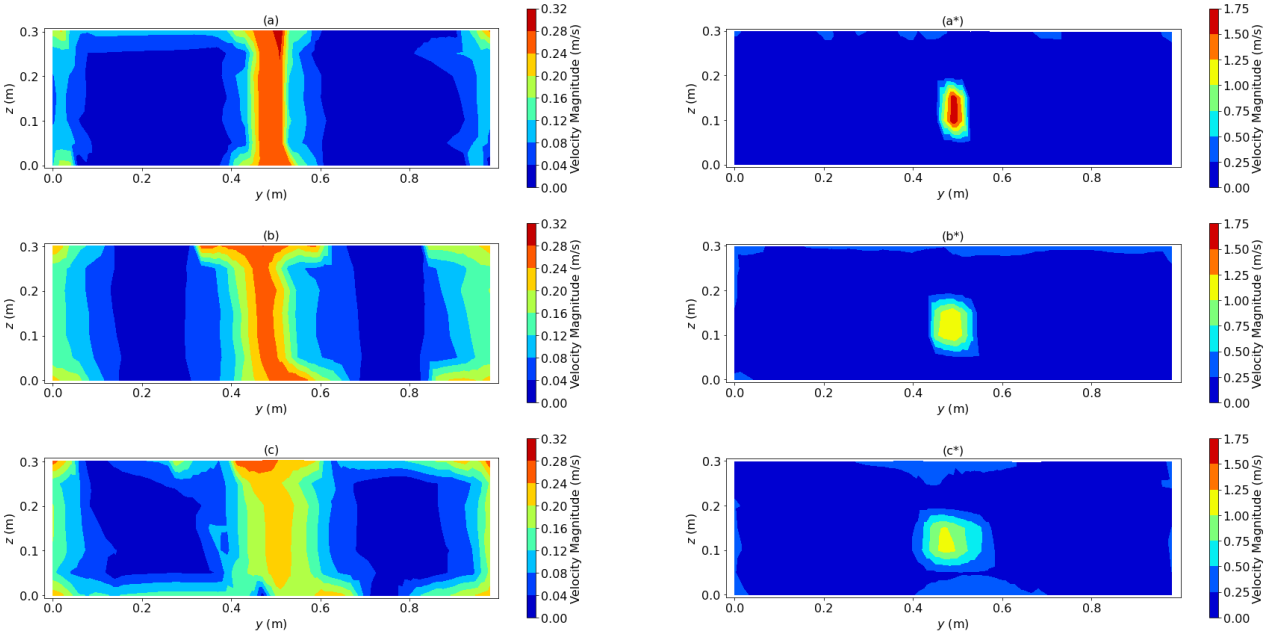


**Fig. 6.** Two-dimensional (2D) velocity magnitude withTELEMAC-3D numerical simulations for reference case (left) and jet case* (right) at (a) and (a*) at x = 0.1 m, (b) and (b*) at x = 1.0 m, (c) and (c*) at x = 2.0 m. Note that legend is not uniformized for reference and jet cases because of their different velocity magnitude values.

## 4. Conclusion

Scaling reals shallow reservoirs according to the Froude number similarity calls for an important geometrical distortion for majority of reservoirs because of the relatively low water depth compared to the horizontal dimensions. Also, real reservoir shapes could not fit into existing laboratory flume because of technical constraints. However, using data from real reservoirs and existing laboratory experiments, the Froude number and the Friction number, which have a significant impact on the flow patterns, have been retained for the design of new laboratory experiences representative of real cases. Two different inlet boundary conditions have been selected for a rectangular reservoir: free surface rectangular inlet channel (reference case) and a turbulent circular inlet jet. The geometrical parameters have been set considering the laboratory experimental constraints, while the hydraulic parameters (flow discharge, water depth) have been set to enhance the maximum and minimum values of Friction number and Froude number considering the experimental limits. Three dimensional (3D) numerical pre-simulations using TELEMAC-3D have been performed, showing the difference of velocity pattern and magnitude between the two cases. A more detailed analysis of turbulent kinetic energy is necessary to understand well the turbulence developed in the jet case.

**Acknowledgements**

This work is partially funded by Association Nationale de Recherche et de la Technologie (ANRT) [CIFRE #2019/1262].

**References**

Abbott D, Kline S (1962) Experimental investigation of subsonic turbulent flow over single and double backward facing steps, Journal of Basic Engineering, 84, 317-325.
Adamsson A, Bergdahl L, Lyngfelt S (2005) Measurement and three-dimensional simulation of flow in a rectangular detention tank, Urban Water Journal, 2(4), 277-287.
Camnasio E, Erpicum S, Orsi E, Pirotton M, Schleiss AJ, Dewals B (2013) Coupling between flow and sediment deposition in rectangular shallow reservoirs, Journal of Hydraulic Research, 51(5), 535-47.
Cherdron W, Durst F, Whitelaw J (1978) Asymmetric flows and instabilities in symmetric ducts with sudden expansions, Journal of Fluid Mechanics, 84,13-31.
Choufi L, Kettab A, Schleiss AJ (2014) Effet de la rugosité du fond d'un réservoir rectangulaire à faible profondeur sur le champ d'écoulement, La Houille Blanche, 83-92.
Claude N, Secher M, Deng J, Valette E, Duclercq M (2019) 2D and 3D numerical modelling of the flow and sediment transport in shallow reservoirs: application to a real case, XXVIth Telemac & Mascaret User Club.
Dufresne M (2008) La modélisation 3D du transport solide dans les bassins en assainissement : du pilote expérimental à l'ouvrage réel (3D modeling of solid transport in waste water basins: from experimental pilot to real reservoir), Doctoral dissertation, Université Louis Pasteur, Strasbourg, France.

Dufresne M, Dewals B, Erpicum S, Archambeau P, Pirotton M (2010) Classification of flow patterns in rectangular shallow reservoirs, Journal of Hydraulic Research, 48(2), 197-204.
Durst F, Melling A, Whitelaw J (1974) Low Reynolds number flow over a plane symmetrical sudden expansion, Journal of Fluid Mechanics, 64, 111.
Fischer H, List J, Koh C, Imberger J, Brooks N (1979) Mixing in inland and coastal waters, Academic Press, 512 pp.
Jirka GH (2004) Integral Model for Turbulent Buoyant Jets in Unbounded Stratified Flows. Part I: Single Round jet, Environmental Fluid Mechanics, 4, 1-56.
Kantoush SA (2008) Experimental study on the influence of the geometry of shallow reservoirs on flow patterns and sedimentation by suspended sediments, Doctoral dissertation, Laboratoire de Constructions Hydrauliques, EPFL, Switzerland.
Mizushima J, Shiotani Y (2001) Transitions and instabilities of flow in a symmetric channel with a suddenly expanded and contracted part, Journal of Fluid Mechanics, 434, 355-369.
Peltier Y, Erpicum S, Archambeau P, Pirotton M, Dewals B (2014) Experimental investigation of meandering jets in shallow reservoirs, Environmental Fluid Mechanics, 14(3), 699-710.
Schleiss AJ, Franca MJ, Juez C, De Cesare G (2016), Reservoir Sedimentation, Journal of Hydraulic Research, 54, 595-614.
Stovin VR, Saul AJ (1994) Sedimentation in Storage Tank Structures, Water Science and Technology, 29, 363-37.